Study of the coupling between real gas effects and rarefied effects on hypersonic aerodynamics

Song Chen, Yuan Hu, and Quanhua Sun

Citation: AIP Conference Proceedings **1501**, 1515 (2012); doi: 10.1063/1.4769718
View online: http://dx.doi.org/10.1063/1.4769718
View Table of Contents: http://scitation.aip.org/content/aip/proceeding/aipcp/1501?ver=pdfcov
Published by the AIP Publishing

Study of the Coupling between Real Gas Effects and Rarefied Effects on Hypersonic Aerodynamics

Song Chen, Yuan Hu, and Quanhua Sun[a]

State Key Laboratory of High Temperature Gas Dynamics
Institute of Mechanics, Chinese Academy of Sciences, Beijing 100190, China
[a]Email: qsun@imech.ac.cn

Abstract. Hypersonic vehicles travel across the atmosphere at very high speed, and the surrounding gas experiences complicated physical and chemical processes. These processes produce real gas effects at high temperature and rarefied gas effects at high altitude where the two effects are coupled through molecular collisions. In this study, we aim to identify the individual real gas and rarefied gas effects by simulating hypersonic flow over a 2D cylinder, a sphere and a blunted cone using a continuum-based CFD approach and the direct simulation Monte Carlo method. It is found that physical processes such as vibrational excitation and chemical reaction will reduce significantly the shock stand-off distance and flow temperature for flows having small Knudsen number. The calculated skin friction and surface heat flux will decrease when the real gas effects are considered in simulations. The trend, however, gets weakened as the Knudsen number increases. It is concluded that the rarefied gas effects weaken the real gas effects on hypersonic flows.

Keywords: Hypersonic flow, Real gas effects, Rarefied gas effects, Coupling mechanism.
PACS: 47.40.Ki, 47.45.-n

INTRODUCTION

Hypersonic vehicles are generally designed to fly or cruise at high altitude with very high speed. The high speed of the vehicle will heat the surrounding air and thus changes the gas properties. Specifically, the hypersonic flows around the vehicle are usually characterized by the presence of strong shocks and equilibrium or non-equilibrium gas chemistry, which is termed in literature as "high-temperature gas effects" or "real gas effects" [1]. The high altitude of the flight will cause another effect called "rarefied gas effects" due to the low density of the air. The rarefied gas effects will appear locally or globally depending on the flight altitude and bluntness radius of the vehicle. The real gas and rarefied gas effects will change the flow properties and even the aerodynamics of the vehicles. Thus accurate prediction of these effects is critical to the design of any vehicle that flies at hypersonic velocity [1].

However, there seems some ambiguity in literature on the definition of these effects. The term "real gas effects" was introduced into aerodynamics in the 1950s, when aerodynamicists were confronted with the complex physical-chemical process caused by hypersonic reentry. Although it differs with the "real gas" definition in classical physical chemistry, this term continues to be widely used nowadays. Some researchers, such as Anderson [2], argue that "high-temperature effects" should be more accurate for description of the effects related to hypersonic reentry. However, the term "real gas effects" has already formed its specific connotation, which refers to the vibrational excitation, dissociation, and even ionization phenomena with the air during hypersonic flight, and has nothing to do with the narrowly-defined sense in traditional physical chemistry textbook. Therefore, the use of real gas effects in hypersonic realm would not create confusion.

Similar to the real gas effects, rarefied gas effects can not find a strict definition either. Early work on rarefied gas effects can be traced to the latter half of the nineteenth century. Maxwell (1887) first pointed out from kinetic point of view that the "non-slip boundary condition" in continuum theory is not always the truth, the temperature jump and velocity slip at the wall will become significant under certain situation [3]. Sherman further illustrated that the continuum theory starts to fail near the wall as the flow became rarefied [4]. Early studies on rarefied gas are mostly focused on the boundary condition and wall properties in the slip flow regime. Later, researchers start to refer the phenomena like temperature jump and velocity slip caused by gas rarefaction as "rarefied gas effects", also known as "rarefied effects" or "rarefaction effects".

It is clear that the real gas effects include the vibrational excitation, dissociation, ionization, radiation, and chemical reactions. These phenomena can be modeled under the frame of continuum theory. Non-equilibrium

28th International Symposium on Rarefied Gas Dynamics 2012
AIP Conf. Proc. 1501, 1515-1521 (2012); doi: 10.1063/1.4769718

thermal and chemical relaxation is related to the rate of its process, which is directly subjected to the collision frequency, and is not the same concept of the actual degree of vibrational excitation and chemical reaction. The relaxation effects are sometimes termed as "non-equilibrium real gas effects", which is not an intrinsic part of real gas effects. The relaxation process, on the other hand, has the flavor of the rarefied gas effects since both depend on intermolecular collisions to reach an equilibrium state during a time period. From the molecular standpoint, the molecular velocity will not follow the Maxwellian distribution when the flow characteristic time is comparable to molecular mean collision time. Thus the flow cannot be modeled under the frame of continuum theory. Since both the real gas effects and rarefied gas effects exist in hypersonic rarefied flows, it becomes very difficulty to model the flow numerically.

In this study, we aim to identify the individual real gas and rarefied gas effects and also the coupling effects on aerodynamics of several simple flying objects. In order to ensure the physical validity and numerical efficiency, a continuum-based computational fluid dynamics (CFD) method and the direct simulation Monte Carlo (DSMC) method are employed. The methodology for the study is explained in the next section. Result and discussion is given thereafter, followed by some concluding remarks at the end of the paper.

METHODOLOGY

As discussed in the previous section, the real gas effects are mainly the high temperature effects, whereas the rarefied gas effects are the high altitude effects in hypersonic flights. Therefore, the real gas effects could be investigated at different flow regime or Knudsen (*Kn*) number. For small Kn flows, real gas effects can be isolated from rarefied gas effects since the latter could be neglected. For larger Kn flows, the real and rarefied gas effects are coupled. One strategy is to run one kinetic simulation and one continuum-based simulation thus to separate the rarefied effects from real gas effects. However, it is very challenging to do this since non-equilibrium real gas effects and rarefied effects are tangled regarding to relaxation. Another strategy is to compare valid results at two different Kn numbers. This approach is not perfect, but is an easy way, which is adopted in this study. Namely, hypersonic flows over vehicles are simulated using a continuum-based CFD approach at a small Kn number by treating the gas as ideal or real. Then similar flows will be simulated using the DSMC method at a larger Kn number. The difference between ideal and real gas cases can be different at the two Kn numbers, which could be explained as the results due to the rarefied gas effects.

The continuum-based CFD approach is a finite volume method solving the Navier-Stokes equations with thermo-chemical nonequilibrium capabilities included. It is solved using a fully coupled, implicit scheme based on Roe's flux-difference splitting algorithm. The finite-rate air chemistry is modeled using a five-species (N_2, O_2, NO, N, O) Park model [5]. The temperature in this study is below 6000K, so ionization and radiation is neglected. The viscosity of each species is calculated using kinetic theory based on collision integral whereas thermal conductivity is calculated using the Eucken relation. The viscosity and thermal conductivity of the mixture are determined using the Wilke's law. For diffusion, the Fick's law is assumed and a constant Schmidt number of 0.5 is used for all species. For thermal non-equilibrium, the energy exchange rate between vibrational and translational modes is determined using the Landau-Teller model. Model details and related coefficients can be found in literature such as Anderson [2] and Park [5]. The code has been extensively used to simulate hypersonic flows in the case of ideal gas [6]. In addition, five-species viscous calculation (5km m/s, 60km altitude) is performed for flow over a cylinder and the results agree well with those in literature [7].

For DSMC simulation, the standard DSMC method [8] is implemented in our in-house code. The variables hard sphere (VHS) molecular model is employed in this study. The internal energy exchange is modeled using the Borgnakke and Larsen model. The chemistry model is based on the commonly used Total Collision Energy (TCE) model with a modified Arrhenius rate coefficient.

It will be hard to investigate the real and rarefied gas effects on a geometrically complicated hypersonic vehicle. Fortunately, both effects become severe in the leading edge domain where 2D cylinder or sphere characters the vehicle forehead. Therefore, hypersonic flows over cylinder or sphere will be studied first, and the aerodynamics of a blunted cone will be investigated thereafter.

Recent study carried out by Ivanov and collaborators showed that the continuum-based CFD techniques can be applied successfully for cylinder flow to *Kn* of below 0.1, or to the limit of the order of 0.01 without slip boundary condition [9], where *Kn* is defined as the ratio of free-stream mean free path λ_∞ to the cylinder radius *R*. With this in mind and to avoid uncertainty from implementation of slip boundary condition, the continuum-based CFD approach is applied to cases having *Kn*<0.01, and the rest cases are simulated using the DSMC method.

The radii of cylinder and sphere are both 0.025m. The semi-angle and length of the blunted cone are $\theta=8^0$ and $L=40R$, respectively. The free stream Mach number (*Ma*) is fixed to 10, the Knudsen number is adjusted by changing the free stream density. The free stream temperature is set to be 223K whereas the wall temperature is fixed at 300K for the blunted cone case and 1000K for the cylinder and sphere cases. Since aerodynamic heating is very sensitive to the grid, grid refinement is strictly performed so that the presented results are grid independent [10]. Specifically, for the CFD simulations, the surface grid Reynolds number is less than 5 and the coarsening ratio between neighboring levels is less than 1.1. For the DSMC simulations, the cell size or the size of sub-cell is less than one third of the local mean free path of gas molecules.

RESULTS AND DISCUSSION

Hypersonic flows over a 2D cylinder, a sphere or a blunted cone are simulated using either CFD or DSMC method. The results in this section are nondimensionlized unless specified otherwise.

Real Gas Effects on Flow Fields

In order to investigate the real gas effects on hypersonic flows, the flow Knudsen number is set at 0.001 to avoid rarefied gas effects. For small Knudsen number flows, Reynolds number is another meaningful parameter, which denotes the viscous effects. The Reynolds number can be calculated directly through the relation:

$$\mathrm{Re} \propto \frac{Ma}{Kn}. \tag{1}$$

Figure 1 shows the results from flow over a 2D cylinder. For ideal gas, there is no vibrational excitation and the number of degrees of freedom is 5, so the ratio of specific heats γ is fixed at 1.4. When the vibrational energy is excited, the ratio of specific heat will change with the flow temperature. Here the flow is assumed equilibrium. For one-temperature and two-temperature model cases, chemical reactions are included in the simulation. The vibrational temperature is assumed the same as the translational and rotational temperature in the 1-T model whereas the vibrational temperature is different in the 2-T model. Fig. 1(a) compares the translational temperature contours obtained using the ideal gas model and 2-T model. Clearly, physical processes such as vibrational excitation, chemical reaction reduce significantly the shock stand-off distance Δ and the translational temperature T_{tr} in the shock layer. For this small *Kn* case, the Reynolds number is large and thus the viscous effect has little impact on the flow patterns. It is known from the inviscid theory that shock stand-off distance will decrease when the ratio of specific heats decreases or the heat capacity (C_V) increases, which is based on the fact that the internal energy of a gas is proportional to C_V at a given temperature. Therefore, the dashed line in Fig. 1(b) for the variable γ case has smaller stand-off distance and lower temperature compared to those in the ideal gas case. Also, to breakup chemical bonds of oxygen and nitrogen molecules, it will consume considerable amount of energy through dissociation

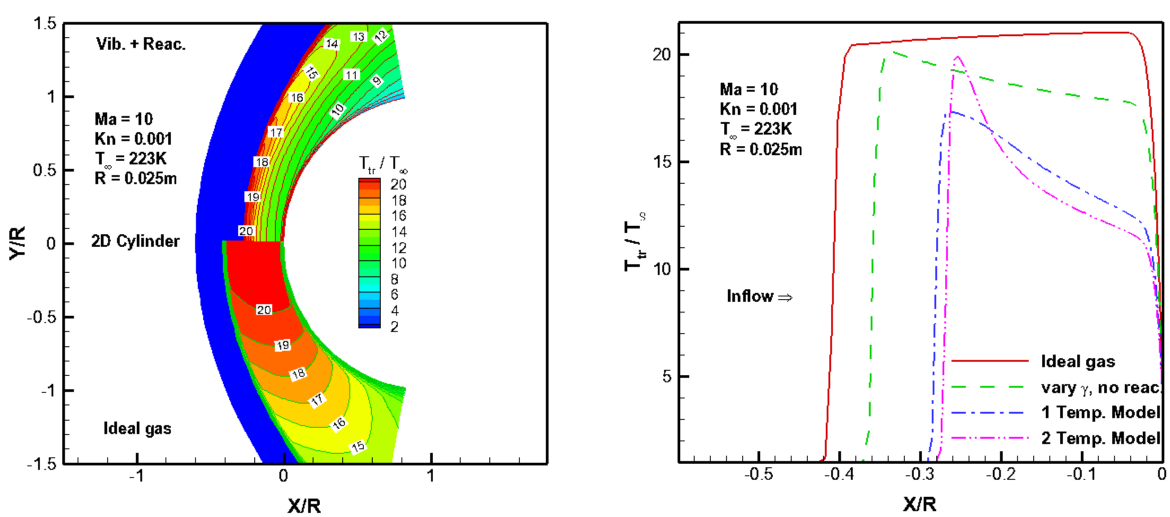

(a) (b)

FIGURE 1. Real gas effects on the translational temperature for the 2D cylinder case when *Ma*=10 and *Kn*=0.001. (a) Temperature contours, (b) distribution of temperature along the stagnation line.

reactions, which will further contribute to the decrease of shock standoff distance and temperature as shown in Fig. 1(b).

The corresponding sphere case is shown in Fig. 2 where 2D cylinder and sphere results are compared. It turns out that the main features of the flows are the same, but the 3D effects in sphere case are obvious. First, the shock stand-off distance in the sphere case is much smaller than the cylinder case, which is typical because the 3D flow has to move closer to the wall to satisfy the continuity equation. Second, the vibrational temperature in the sphere case is slightly higher than the 2D case. However, the atomic oxygen mass fraction seems about the same for the two cases.

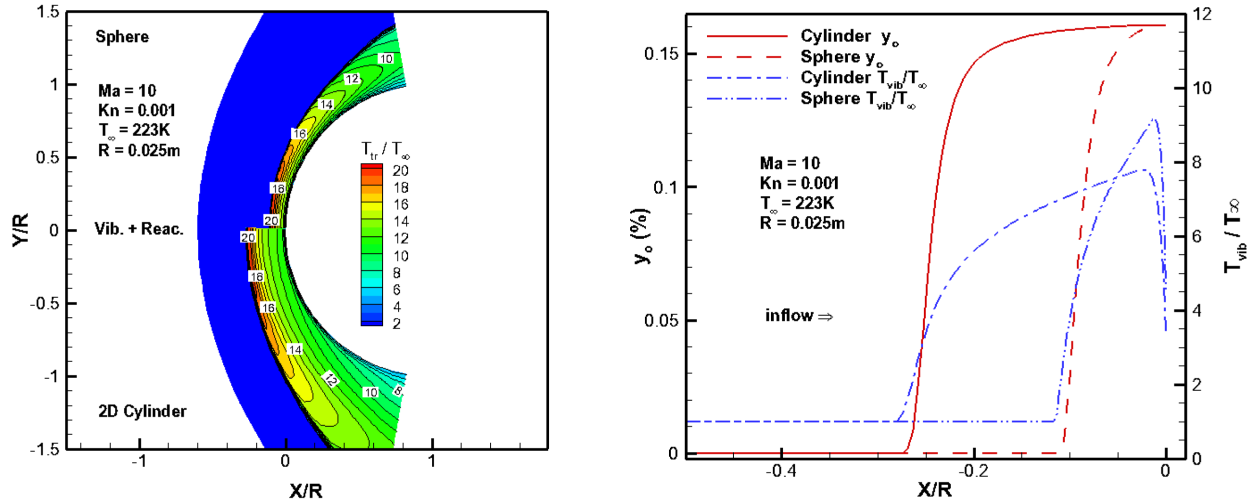

(a) (b)

FIGURE 2. Comparison of the 2D cylinder and sphere results with real gas effects when *Ma*=10 and *Kn*=0.001. (a) Translational temperature contours, (b) atomic oxygen mass fraction and vibrational temperature distribution along the stagnation line.

Rarefied Gas Effects on Flow Field

As *Kn* increases, the molecular mean free path becomes comparable to the cylinder radius and the continuum theory will fail eventually. Figure 3(a) shows the translational temperature contours for flow over a cylinder when *Kn*=0.01 and 0.1, and Fig. 3(b) shows the temperature component distributions along the stagnant line. It is clear that the translational temperature at *Kn*=0.01 is more closer to the *Kn*=0.001 case than the *Kn*=0.1 case. Rarefied gas effects start to be important at *Kn*=0.1. The flow pattern is essentially different between the *Kn*=0.01 case and *Kn*=0.1

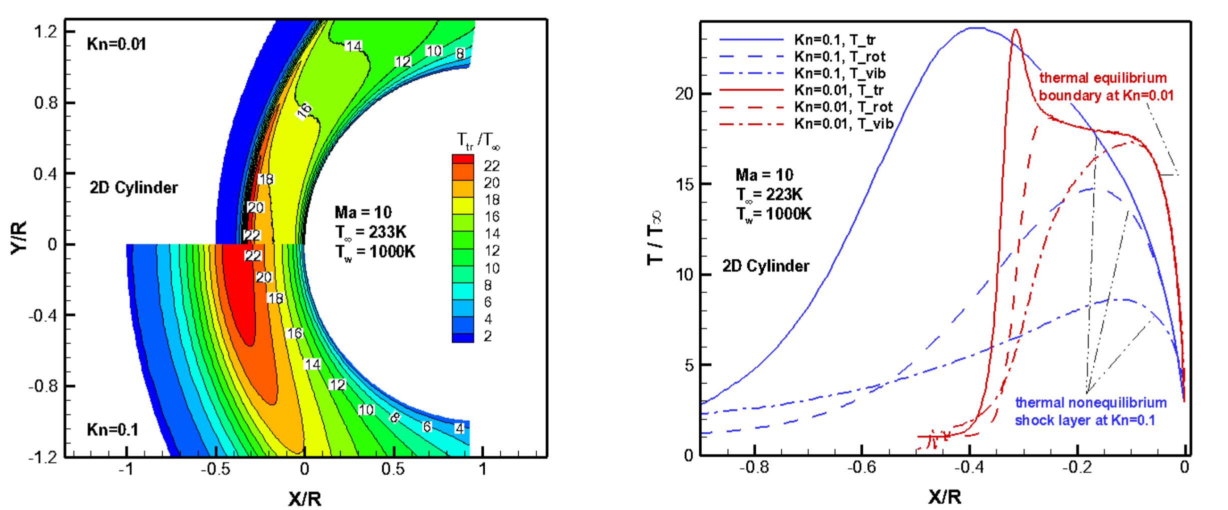

(a) (b)

FIGURE 3. Knudsen number effects on the temperature for the 2D cylinder case when *Ma*=10. (a) Temperature contours, (b) distribution of temperature along the stagnation line.

case. When the flow is rarefied, the shock loses its discernable structure and merges with the boundary layer. For *Kn*=0.01, there is strong thermal non-equilibrium behind the shock. However, temperatures of three modes can finally reach its equilibrium state in the boundary layer. The difference among the temperatures will increase as *Kn* increases. For *Kn*=0.1, the thermal non-equilibrium almost spreads throughout the entire flow region in the leading edge vicinity.

The flow patterns are similar in the sphere case except that the shock stand-off distance is smaller as illustrated in Fig. 4. The main difference is that the sphere case exhibits stronger non-equilibrium features at the same Knudsen number. At *Kn*=0.01, the difference between maximum T_{tr} and T_{vib} is about 40%, compared to 25% in the 2D cylinder case. This difference further increases when *Kn*=0.1. This phenomenon may be attributed to the shorter shock stand-off distance which prevents the flow to reach equilibrium.

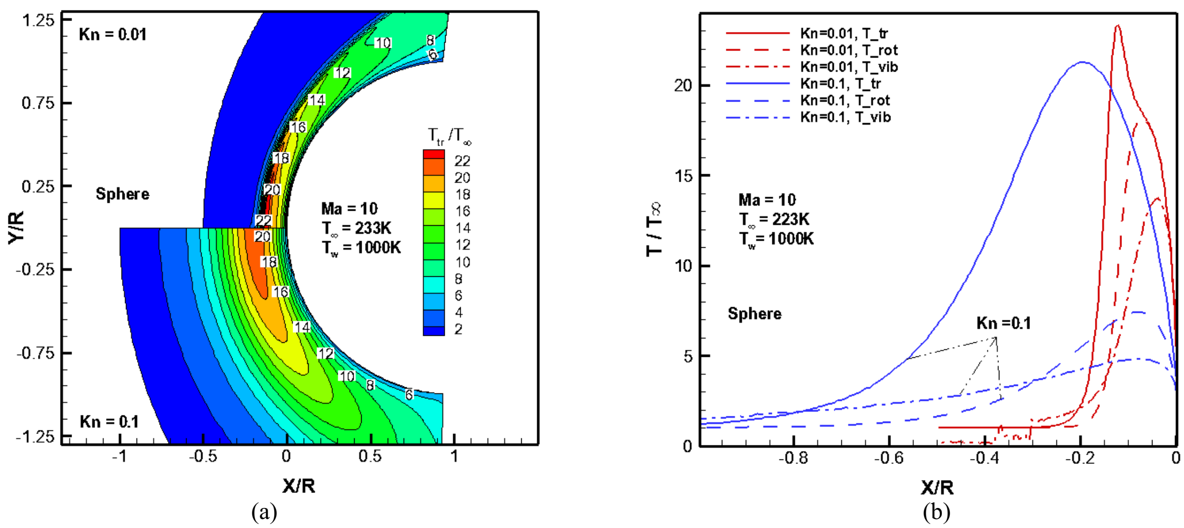

FIGURE 4. Knudsen number effects on the temperature for the sphere case when *Ma*=10. (a) Temperature contours, (b) distribution of temperature along the stagnation line.

Coupling Effects on Aerodynamics

The aerodynamics considered here are the surface pressure, skin friction and surface heat flux. They are non-dimensionalized as pressure coefficient C_p, skin friction coefficient C_f, and the Stanton number C_h:

$$C_f = \frac{\tau_w}{\rho_\infty V_\infty^2/2}, \quad C_p = \frac{p_w - p_\infty}{\rho_\infty V_\infty^2/2}, \quad C_h = \frac{q_w}{\rho_\infty V_\infty (H_\infty - H_w)}. \tag{2}$$

Figure 5 shows the distributions of C_f, C_h and C_p along the surface for both the cylinder and sphere cases at two *Kn* numbers. As the angle θ (clockwise to the x axis) increases along the surface, the skin-friction coefficients grow non-monotonous with a peak at about 45 degree. When *Kn*=0.01, the C_f predicted with the ideal gas model is about

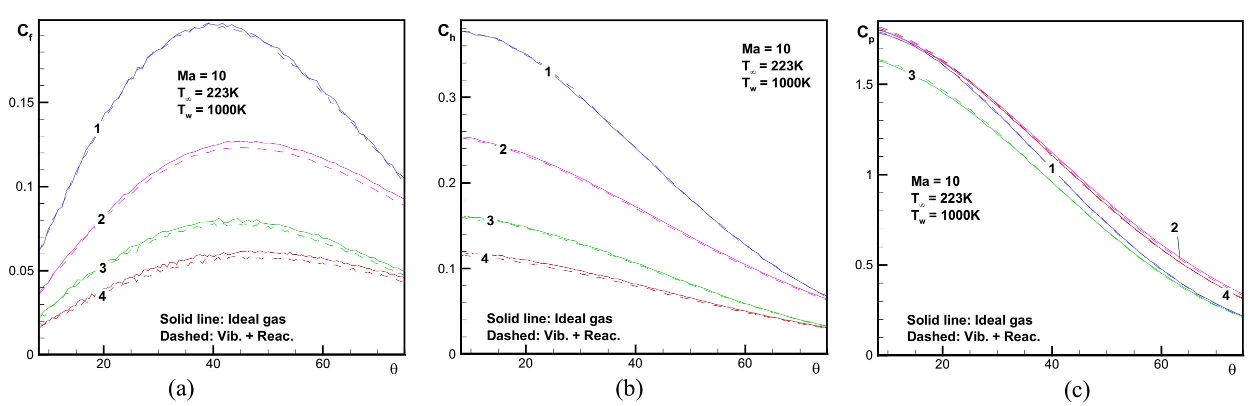

FIGURE 5. Real gas effects on the surface properties for cylinder or sphere case where 1-sphere, kn=0.05; 2-cylinder, kn=0.05; 3-sphere, kn=0.01; 4-cylinder, kn=0.01. (a) Skin friction coefficient, (b) Stanton number, (c) pressure coefficient.

3.5% higher than with the real gas effects for the cylinder case. This difference decreases as *Kn* is increased to 0.05, which implies a coupling between the real gas and rarefied gas effects. The skin friction on the sphere is larger than on the cylinder and is less sensitive to the real gas effects. The behavior of real and rarefied gas effects on the Stanton number is similar to it on the skin friction only that the difference due to real gas effects becomes smaller. For the pressure coefficient, it is found that the impact of real gas effects is negligible, and the difference of the surface pressure between cylinder and sphere is rather small.

Finally we simulate two cases for flows over a blunted cone that is a projectile body when *Kn*=0.003 and *Kn*=0.03. Here the Knudsen number is evaluated based on the nose radius. When *Kn*=0.003, it is hard to see the difference between the overall temperature flow field (Fig. 6(a)) obtained using the ideal gas and real gas models. However, slight difference is observed on the surface heat flux (Fig. 6(b)) and skin friction (Fig. 6(d)), which is not surprised since the flow in the nose area should be the same as flow over a sphere under the same free stream condition. When the real gas effects are included in the simulation, the stagnant heat flux on the blunted cone is reduced about 8% at *Kn*=0.003, and the effect diminishes along the cone arc. Compared to the surface heat flux, the reduction on the skin friction due to real gas effects can be hardly seen near the stagnation point, but becomes apparent downstream with a difference about 8% for the major part of the surface. Thus, the impacts of real gas effects are mainly near the leading edge region on the surface heat flux but extend to a wider region on the skin friction. When *Kn* increases to 0.03, the rarefied gas effects seem to restrict the real gas effects as both the heat flux and skin friction are almost unchanged with or without the real gas effects. For the surface pressure, the real gas effects are negligible, which is similar to the cylinder or sphere case.

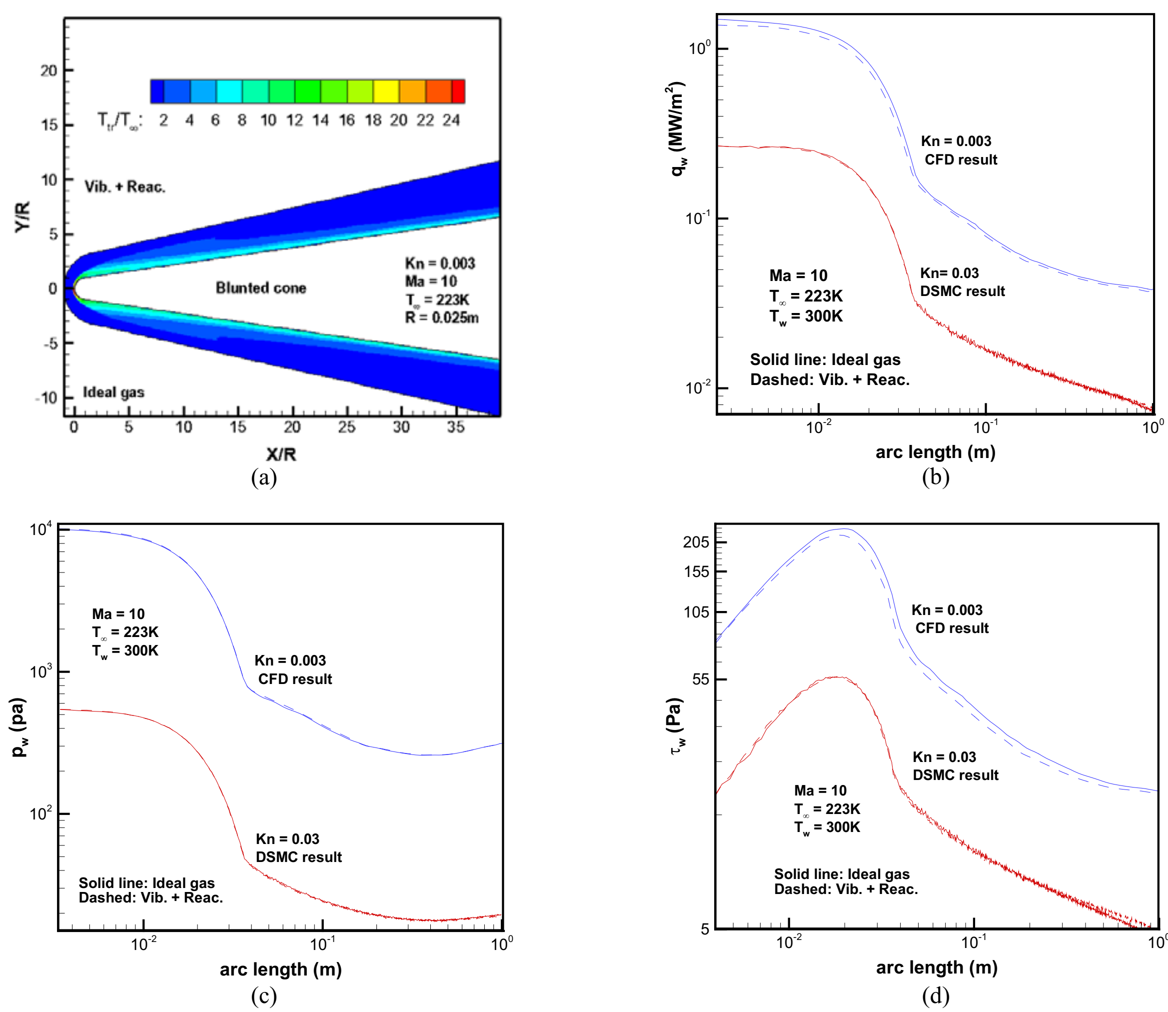

FIGURE 6. Real gas effects on the blunted cone when *Kn*=0.003 and *Kn*=0.03 with *Ma*=10. (a) Translational temperature contours at *Kn*=0.003, (b) heat flux distribution, (c) surface pressure distribution, (d) skin-friction distribution.

CONCLUDING REMARKS

Based on the simulation results, some conclusions can be drawn as follows:

1. Physical processes such as vibrational excitation and chemical reaction will reduce significantly the shock stand-off distance and flow temperature for hypersonic flows having small Knudsen number.

2. With real gas effects included, the predicted aerodynamics of vehicles such as skin friction and surface heat flux are smaller than those using the ideal gas model. This trend gets weakened as the Knudsen number increases. The surface pressure, however, is insensitive to the gas model.

It is reasonable to argue that the real gas effects are weakened by the rarefied gas effects as the Knudsen increases. The physical mechanism of this coupling can be explained as follows. There are two means to reduce vibrational excitation or chemical reaction when the flow gets rarefied or the flight altitude increases. First, high altitude means low density thus causes the reduction of reaction rate through the concentration of the reactants. Second, the flow temperature decreases as flow gets rarefied, then the reaction rate constant will decrease, which further reduces the reaction rates.

Generally speaking, when the flow is rarefied or the total temperature is not very high, the real gas effects have little impact on vehicle's aerodynamics although the flow field will have obvious change. Of course, the impact is expected to be more significant if the flow Mach number increases. In this case, ionization or even radiation should be taken into account in numerical simulations.

ACKNOWLEDGMENTS

The authors would like to acknowledge the support from the National Natural Science Foundation of China with grants 91116013 and 11111120080.

REFERENCES

1. J. J. Bertin and R. M. Cummings, *Annu. Rev. Fluid Mech.* **38**, 129-157 (2006).
2. J. D. Anderson, *Hypersonic and High Temperature Gas Dynamics*, New York: McGraw-Hill Book Company, 1989.
3. M. N. Kogan, *Annu. Rev. Fluid Mech.* **5**, 383-404 (1973).
4. F. S. Sherman, *Annu. Rev. Fluid Mech.* **1**, 317-340 (1969).
5. C. Park, *Nonequilibrium Hypersonic Aerothermodynamics*, New York: John Wiley and Sons, Inc., 1990.
6. H. Zhu, G. Wang, Q. Sun, and J. Fan, *Acta Aerodynamica Sinica*, (in press) (2012).
7. J. R. Edwards, *J. Comput. Phys.* **123**, 84-95 (1996).
8. G. A. Bird, *Molecular Gas Dynamics and the Direct Simulation of Gas Flows*, Oxford: Clarendon Press, 1994.
9. M. S. Ivanov, D. V. Khotyanovsky, A. A. Shershnev, A. N. Kudryavtsev, A. A. Shevyrin, S. Yonemura, and Y. A. Bondar, *Thermophys. and Aeromech.* **18**, 523-534 (2011).
10. Q. Sun, H. Zhu, G. Wang, and J. Fan, *Theor. Appl. Mech. Lett.* **1**, 022001 (2011).